COMPUTER ENGINEERING

UDC 621.375 (045)
DOI:10.18372/1990-5548.69.16423

[1]V. V. Chikovani,
[2]S. V. Golovach

A VIBRATORY GYROSCOPE SCALE FACTOR AND BIAS ON-RUN SELF-CALIBRATION

[1]Aerospace Control Systems Department, National Aviation University, Kyiv, Ukraine
[2]JSC Elmiz, Kyiv, Ukraine
E-mails: [1]v_chikovani@ukr.net ORCID 0000-0003-1436-7180
[2]golovach.s@meta.ua ORCID 0000-0001-6786-3781

Abstract*—A new method for on-run periodic scale factor and bias self-calibration of vibratory gyroscopes in an inertial measurement unit with a redundant number of sensors is proposed. Self-calibration uses predefined virtual positive and negative angle rates to calibrate the SF, and the bias of the gyroscope that is in calibration mode, while the others, at least three gyroscopes of an inertial measurement unit, whose sensitivity axes do not lie in the same plane, operate in the measurement mode to measure the real angle rate of a vehicle. The projection of the current angle rate onto the sensitivity axis of the gyroscope being calibrated is computed from the results of measuring the full angle rate vector by the other three gyroscopes, creating conditions for the calibration procedure. In contrast to known methods, such as single-axis or multi-axis rotation of an inertial measurement unit and vibration modes reversal, the proposed method does not use mechanical rotation, which requires additional devices, and does not require a reorientation of the vibrating wave, which entails the need to align the parameters of the two measuring channels. The scale factor and bias calibration procedure using this method is the same for any gyroscope of an inertial measurement unit and can be applied to several gyroscopes at the same time. Therefore, the proposed method has great potential for an application not only for small-sized 4-gyro inertial measurement unit based on vibratory gyroscopes but also for multi-gyro inertial measurement unit based on micro-electro-mechanical gyroscopes. Experimentally shown that using the proposed method a gyro requirements mitigation coefficient can be substantially increased and can provide high accuracy for autonomous navigation systems based on low-cost, small-sized, and micro-electro-mechanical gyroscopes.*

Index Terms—Scale factor; drift; virtual angle rate; self-calibration; requirements mitigation coefficien.t.

I. INTRODUCTION

Gyroscope errors have a significant influence on inertial navigation system (INS) accuracy. For INS based on low-cost gyroscopes, position and attitude errors accumulate very quickly over time [1], [2]. For example, the position errors of a low-cost micro-electro-mechanical systems (MEMS)-gyro-based INS will grow to kilometers for several minutes of a motion time [3]. Independent on which gyros are used in an INS, to improve performance of INS built on lower cost gyros, there is a need to restrict the fast accumulation of errors versus time. This problem is relevant not only for MEMS gyroscopes but also for small-sized gyroscopes of all types, such as fiber-optic, ring laser, and Coriolis vibratory gyroscopes (CVG) to build an autonomous low-cost, high-accurate INS. Among the types listed above gyroscopes, CVGs have advantages in terms of reliability and low cost, as well as, as will be shown in this work, of the ability to perform calibration without the use of additional rotary devices and calibration maneuvers of a vehicle.

II. ANALYSIS OF PUBLICATION DATA AND PROBLEM STATEMENT

There are some methods to improve INS performance. First, a very popular method of INS and a global positioning system (GPS) receiver integration should be mentioned. Inertial navigation system data and high accurate GPS position data are being combined in a Kalman filter that estimates gyro errors based on the accepted models [4] – [6]. However, receiving a GPS signal is highly dependent on environmental conditions, and it is not always possible. Therefore, there is a time gap when an INS must operate in autonomous mode with a fast accumulation of gyro errors.

The second method is a self-calibration one using single-axis [7] or multi-axis [8] – [10] mechanical rotation of inertial measurement unit (IMU). Those autonomous methods enable one to calibrate gyros

© National Aviation University, 2021

and accelerometers biases, scale factors (SF), and their misalignments without the involvement of external information.

To identify the thermal model, the rotation scheme is repeated ten times to estimate error parameters under different temperatures. Then, the Kalman filter algorithm is used to estimate parameters, which are under calibration. These methods propose to mount an IMU on the two- or three-dimensional gimbal that increases system complexity, power consumption, size, cost and reduces reliability, as well.

The third method is a periodic self-calibration of gyro biases and SFs in IMU without mechanical rotation. This method uses IMU based on a redundant number of CVGs including MEMS gyros, by reversing vibration modes. In such an IMU there must always be three gyros whose sensing axes do not lay on one plane and can measure full (three-dimensional) vector of vehicle angle rate while at least one gyro is in calibration mode [11] – [13]. The periodic switching between the vibration modes limits the bandwidth of the gyroscope and causes transient. Moreover, it reduces calibration effectiveness under temperature change.

III. Review Purpose and Tasks of the Research

This paper presents a new method to implement periodic self-calibration of CVGs biases and SFs in the IMU with redundant gyroscopes without mechanical rotation and modes reversal. The method does not change gyro bandwidth and be more efficient under temperature change. The idea of the proposed method is that instead of modes reversal or mechanical rotation, predetermined virtual positive and negative angle rates are used to calibrate SF and bias of a gyro, which is in calibration mode, while the other three gyros of the IMU are in the measurement mode. A projection of the current angle rate on the sensing axis of the gyro being calibrated is computed and removed by the results of measurement of full angle rate vector by the other three gyros, thus creating the conditions for the calibration procedure.

IV. Simulation of a Virtual Angle Rate

To realize the method, gyros in the IMU should be disposed of so that any three gyros would not lay in one plane. One of the known dispositions of the gyros meeting the requirement is a polyhedral truncated pyramid [11].

To simulate the predetermined virtual positive and negative angle rates in a CVG operational temperature range, one should first be built a temperature model that connects the value of the electrical signal (voltage for analog CVG or code for digital one) with the angle rate that should be simulated. This model can be built by analogy with the SF model based on not necessarily only temperature data, but on the resonant frequency, drive amplitude, and quadrature amplitude, as well [14].

Then, using this model, code (or voltage) that simulates the predetermined virtual angle rate is computed and added to the output of controller 3 that controls the Coriolis signal, S_y, presented in Fig. 1 of a CVG control system block diagram [15].

Figure 1 presents a ring-type resonator with eight, symmetrically located through the angle 45 deg, electrodes. Diametrically opposite electrodes are connected to each other. As a result, a sensor has two input signals (X_{in}, Y_{in}) and two output signals (X_{out}, Y_{out}). It means that the sensor can be considered as a two-input-two-output plant.

Vibration excitation is provided by supplying a periodical signal to the X_{in} electrode at the resonant frequency. Response to the excitation is picked off from the X_{out} electrode and is used to sustain vibration and to track for changing of resonant frequency using phase lock loop (*PLL*) with the generation of the two orthogonal sine and cosine signals. Vibration amplitude stabilization at the value of A_0 is based on controller 2. Secondary wave amplitude is picked off from the Y_{out} electrode located at the nodal point of the primary wave and with the help of the sum of negative feedback signals, formed by controllers 3 and 4, is suppressed by supplying opposite phase signal to the Y_{in} electrode located at the other nodal point of the primary wave.

Thus, feedback signal amplitude that compensates for the sine (Coriolis) component S_y of the node vibration is proportional to the angle rate Ω. Hence, when the processor adds the code corresponding to the angle rate Ω_v to the output of controller 3, the gyroscope will simulate the virtual angle rate Ω_v, which is added to the external (real) angle rate.

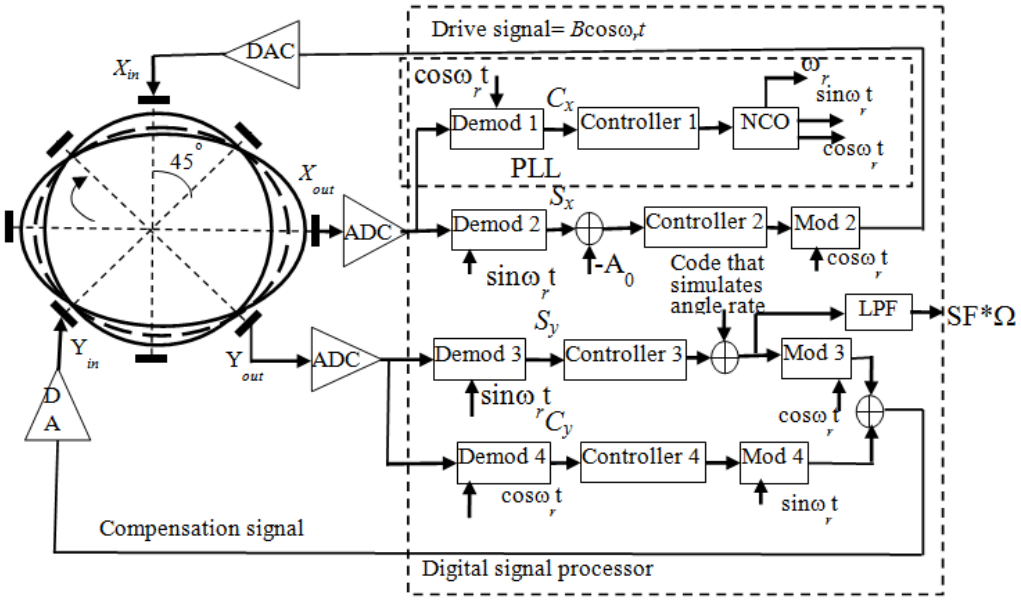

Fig. 1. Coriolis vibratory gyroscopes control system block diagram

At the same time, three other gyroscopes of an IMU measure the current real angle rate acting on the gyro under calibration due to vehicle motion to create the proper conditions for the gyro calibration.

V. Calibration Process and its Analysis

To explain in detail the calibration process of any gyroscope in an IMU, consider, as an example, an IMU consisting of four gyroscopes G_1, G_2, G_3, and G_4 which axes of sensitivity are perpendicular to the faces of the truncated tetrahedral pyramid shown in Fig. 2 [11].

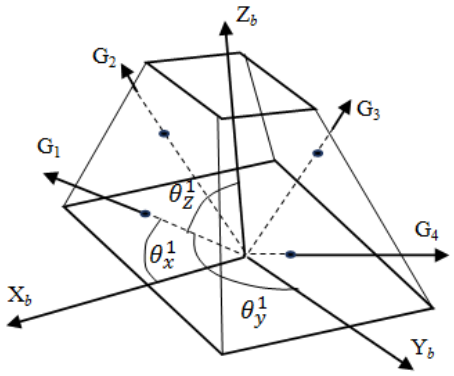

Fig. 2. A redundant-gyro IMU of four single-axis gyros

In this figure, $X_bY_bZ_b$ is the rectangular coordinate system connected with the IMU, which should be aligned with the vehicle axes. The angles $\theta_x^k, \theta_y^k, \theta_z^k$, $k = 1\ldots4$, between the sensing axis of the kth gyroscope and the coordinate system $X_bY_bZ_b$ are supposed to be known. These angles are usually determined in the process of the IMU calibration at the manufacturer's site.

Figure 2 shows the angles for only the first G_1 gyroscope. In this IMU of four gyroscopes, only one gyroscope can be entered into the calibration mode, while the other three gyroscopes have to operate in the angle rate measurement mode to measure the full, three-dimensional, angle rate vector of a vehicle.

The process of SF and bias calibration by this method is the same for any of the IMU gyroscopes. Therefore, this procedure is considered for only the first gyro G_1, presented in Fig. 2.

Figure 3 presents a block diagram of each gyro in the IMU. The block diagram includes a gyroscope 1 itself, a unit 2 used to generate a signal that simulates constant, but sign-changing predetermined virtual angle rates, a unit 3 averages the output signal of the gyroscope, and switches 4 switch the operating modes of a gyro.

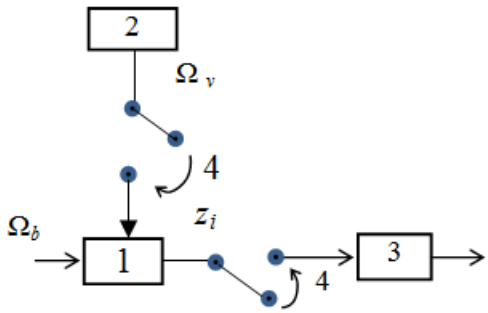

Fig. 3. Each gyro block diagram of the redundant IMU

When both switches 4 are open, a gyroscope 1 is operating in the measurement mode, and when both switches are closed, the gyroscope is operating in the calibration mode.

Under calibration mode, block 2 generates a signal in the form of a digital code, for digital gyroscopes, or voltage, for analog gyroscopes, equivalent to a predetermined virtual angle rate Ω_v for time interval T and adds it to the output signal of the controller 3, shown in Fig. 1. In this case, the gyro output signal is the sum of the virtual angle rate Ω_v and the projection Ω_k (k = 1) of a vehicle angle rate Ω_b on the sensing axis of the kth (first) gyro under calibration.

The total signal $\Omega_1 + \Omega_v$ enters the averaging unit 3 and at its output the averaged over a time interval T signal z_{av}^{+} is formed. Then, block 2 generates a signal $-\Omega_v$ during the same time interval T, and the output of block 3 forms one more averaged over time interval T signal z_{av}^{-}. Under the supposition that both SF and bias of the gyro under calibration are constant values, the following two equations can be written:

$$\begin{aligned} z_{av}^{+} &= \mathrm{SF}_0\left(\Omega_v + \bar{\Omega}_1\right) + B_0, \\ z_{av}^{-} &= \mathrm{SF}_0\left(-\Omega_v + \bar{\Omega}_2\right) + B_0, \end{aligned} \tag{1}$$

where SF_0 is the gyro scale factor; B_0 is the gyro bias; Ω_v is the value of the simulated virtual angle rate; $\bar{\Omega}_1$ is the average value over the first time interval T of the vehicle angle rate Ω_b projection on the sensing axis of the gyro under calibration; $\bar{\Omega}_2$ is the average value over the second time interval T of the vehicle angle rate Ω_b projection on the sensing axis of the gyro under calibration.

Projections $\bar{\Omega}_1$ and $\bar{\Omega}_2$ are computed by the readings of the three gyros, which are in the measurement mode, by the following expressions:

$$\begin{aligned} \bar{\Omega}_1 &= \left(\bar{\Omega}^1_{G2}\cos\theta^2_x + \bar{\Omega}^1_{G3}\cos\theta^3_x + \bar{\Omega}^1_{G4}\cos\theta^4_x\right)\cos\theta^1_x + \left(\bar{\Omega}^1_{G2}\cos\theta^2_y + \bar{\Omega}^1_{G3}\cos\theta^3_y + \bar{\Omega}^1_{G4}\cos\theta^4_y\right) \\ &\quad \cdot\cos\theta^1_y\left(\bar{\Omega}^1_{G2}\cos\theta^2_z + \bar{\Omega}^1_{G3}\cos\theta^3_z + \bar{\Omega}^1_{G4}\cos\theta^4_z\right)\cos\theta^1_z, \\ \bar{\Omega}_2 &= \left(\bar{\Omega}^2_{G2}\cos\theta^2_x + \bar{\Omega}^2_{G3}\cos\theta^3_x + \bar{\Omega}^2_{G4}\cos\theta^4_x\right)\cos\theta^1_x + \left(\bar{\Omega}^2_{G2}\cos\theta^2_y + \bar{\Omega}^2_{G3}\cos\theta^3_y + \bar{\Omega}^2_{G4}\cos\theta^4_y\right) \\ &\quad \cdot\cos\theta^1_y\left(\bar{\Omega}^2_{G2}\cos\theta^2_z + \bar{\Omega}^2_{G3}\cos\theta^3_z + \bar{\Omega}^2_{G4}\cos\theta^4_z\right)\cos\theta^1_z, \end{aligned} \tag{2}$$

where $\bar{\Omega}^1_{G2}$, $\bar{\Omega}^1_{G3}$, and $\bar{\Omega}^1_{G4}$ are the averaged over the first time interval T of a vehicle angle rate Ω_b projections on the gyroscopes G_2, G_3, and G_4 sensing axes, respectively; $\bar{\Omega}^2_{G2}$, $\bar{\Omega}^2_{G3}$, and $\bar{\Omega}^2_{G4}$ are the averaged over the second time interval T of the vehicle angle rate Ω_b projection on the gyroscopes G_2, G_3, and G_4 sensing axis, respectively.

The solution of equations (1), using the measured values $\bar{\Omega}_1$ and $\bar{\Omega}_2$ from (2), for SF_0 and B_0 gives the calibrated values of these parameters:

$$\begin{aligned} SF_0 &= \frac{z_{av}^{+} - z_{av}^{-}}{2\Omega_v + \bar{\Omega}_1 - \bar{\Omega}_2}, \\ B_0 &= \frac{z_{av}^{-}(\Omega_v + \bar{\Omega}_1) + z_{av}^{+}(-\Omega_v + \bar{\Omega}_2)}{2\Omega_v + \bar{\Omega}_1 - \bar{\Omega}_2}. \end{aligned} \tag{3}$$

Thus, to obtain a solution for the parameters being calibrated it needs to simulate two, p = 2, angle rates with opposite signs, when both SF and bias are supposed to be constant during calibration time.

The main determinant of the system (1) should not be equal to zero, i.e.:

$$B_0 = 2\Omega_v + \bar{\Omega}_1 - \bar{\Omega}_2. \tag{4}$$

However, in a real situation, when there is a measurement noise, to ensure satisfactory accuracy, it is desirable to have this determinant as large as possible by absolute value, i.e.

$$\left|2\Omega_v + \bar{\Omega}_1 - \bar{\Omega}_2\right| >> 0. \tag{5}$$

Since the values of $\bar{\Omega}_1$ and $\bar{\Omega}_2$ can be the maximum possible and opposite in sign for the vehicle, which the IMU is mounted on, it is advisable to choose Ω_v from the condition:

$$\left|\Omega_v\right| >> \left|\Omega_{\max}\right|, \tag{6}$$

where $\Omega_{\max}$ is the maximum angle rate of the vehicle.

Therefore, to maximize the determinant of the system (1) at any possible angle rate for the particular vehicle, the virtual angle rate should be much more than the maximum angle rate of this vehicle.

In a practical case, the averaging time interval T should be chosen sufficiently long (some tens of seconds) to reduce measurement noise, then $\bar{\Omega}_1 < \Omega_{\max}$ and $\bar{\Omega}_2 < \Omega_{\max}$. Thus, Ω_v can be chosen of no more than $1.5\Omega_{\max}$ to guarantee that the main determinant will be sufficiently large.

When the ambient temperature does not remain constant, but slowly changes during the calibration process, a linear drift of both bias and scale factor

usually appears. Therefore, linear drift components should be included in SF and bias models. In this case, it is necessary to simulate at least four, $p = 4$, virtual constant angle rate with different signs $+\Omega_v$ and $-\Omega_v$ for each next time interval of T duration to obtain the following four equations:

$$
\begin{aligned}
z_{av}^{+1} &= (SF_0 + \frac{1}{T}\int_0^T a_{SF}tdt)(\Omega_v + \bar{\Omega}_1) + B_0 + \frac{1}{T}\int_0^T a_B tdt,\\
z_{av}^{-2} &= (SF_0 + \frac{1}{T}\int_T^{2T} a_{SF}tdt)(-\Omega_v + \bar{\Omega}_2) + B_0 + \frac{1}{T}\int_T^{2T} a_B tdt,\\
z_{av}^{+3} &= (SF_0 + \frac{1}{T}\int_{2T}^{3T} a_{SF}tdt)(\Omega_v + \bar{\Omega}_3) + B_0 + \frac{1}{T}\int_{2T}^{3T} a_B tdt,\\
z_{av}^{-4} &= (SF_0 + \frac{1}{T}\int_{3T}^{4T} a_{SF}tdt)(-\Omega_v + \bar{\Omega}_4) + B_0 + \frac{1}{T}\int_{3T}^{4T} a_B tdt,
\end{aligned}
\tag{7}
$$

where $z_{av}^1, z_{av}^2, z_{av}^3, z_{av}^4$ are averaged over the four consecutive time intervals of T duration of the simulated, sign-changing virtual angle rate $\pm\Omega_v$; SF_0, B_0 are the scale factor and bias of the gyro under calibration at the beginning of a calibration interval; a_{SF}, a_B are the scale factor and bias linear drift rate, respectively; $\bar{\Omega}_1, \bar{\Omega}_2, \bar{\Omega}_3, \bar{\Omega}_4$ are the averaged over the four consecutive time intervals of T duration of a vehicle angle rate Ω_b projections on the sensing axis of the gyro under calibration, respectively.

After integrating (7), the following matrix equation to determine unknowns SF_0, B_0, a_{SF}, and a_B is obtained:

$$
\begin{pmatrix} z_{av}^{+1} \\ z_{av}^{-2} \\ z_{av}^{+3} \\ z_{av}^{-4} \end{pmatrix} = M \begin{pmatrix} SF_0 \\ a_{SF} \\ B_0 \\ a_B \end{pmatrix}, \tag{8}
$$

where matrix M is

$$
M = \begin{pmatrix}
\Omega_v + \bar{\Omega}_1 & (\Omega_v + \bar{\Omega}_1)\frac{T}{2} & 1 & \frac{T}{2} \\
-\Omega_v + \bar{\Omega}_2 & (-\Omega_v + \bar{\Omega}_2)\frac{3T}{2} & 1 & \frac{3T}{2} \\
\Omega_v + \bar{\Omega}_3 & (\Omega_v + \bar{\Omega}_3)\frac{5T}{2} & 1 & \frac{5T}{2} \\
-\Omega_v + \bar{\Omega}_4 & (-\Omega_v + \bar{\Omega}_4)\frac{7T}{2} & 1 & \frac{7T}{2}
\end{pmatrix}.
$$

When $\det(M) \neq 0$, it is possible to determine the unknown parameters, and when the condition (6) is fulfilled, the determinant has a large enough value and makes it possible to determine these parameters with satisfactory accuracy at high measurement noise. For example, $\det(M) = -1.58\times10^7$ for $\Omega_v = 110$ deg/s, $\bar{\Omega}_1 = \bar{\Omega}_3 = 100$ deg/ s, $\bar{\Omega}_2 = \bar{\Omega}_4 = -100$ deg/ s, $T = 30$ s, and for $T = 10$ s, $\det(M) = -1.76\times10^6$. It means that even at an insignificant excess of Ω_v over vehicle angle rate, a sufficiently high value of $\det(M)$ enables reaching good calibration accuracy for short time.

To determine the parameters SF_0, B_0, a_{SF}, and a_B, redundant measurements can also be used, that can be obtained for SF and bias, B, linear drift models when the number of simulated sign-changing angle rates is $p > 4$. This results in similar to (8) matrix equation written for even n:

$$
\begin{pmatrix} z_{av}^{+1} \\ z_{av}^{-2} \\ \vdots \\ z_{av}^{-p} \end{pmatrix} = M_1 \begin{pmatrix} SF_0 \\ a_{SF} \\ B_0 \\ a_B \end{pmatrix}, \tag{9}
$$

where matrix M_1 is

$$
\begin{pmatrix}
\Omega_v + \bar{\Omega}_1 & (\Omega_v + \bar{\Omega}_1)\frac{T}{2} & 1 & \frac{T}{2} \\
-\Omega_v + \bar{\Omega}_2 & (-\Omega_v + \bar{\Omega}_2)\frac{3T}{2} & 1 & \frac{3T}{2} \\
\vdots & \vdots & \vdots & \vdots \\
\Omega_v + \bar{\Omega}_{p-1} & (\Omega_v + \bar{\Omega}_{p-1})\frac{(2p-3)T}{2} & 1 & \frac{(2p-3)T}{2} \\
-\Omega_v + \bar{\Omega}_p & (\Omega_v + \bar{\Omega}_p)\frac{(2p-1)T}{2} & 1 & \frac{(2p-1)T}{2}
\end{pmatrix}.
$$

The solution of this equation can be obtained, using the least-squares method:

$$
\begin{pmatrix} SF_0 \\ a_{SF} \\ B_0 \\ a_B \end{pmatrix} = (M_1^T M_1)^{-1} M_1^T \begin{pmatrix} z_{av}^{+1} \\ z_{av}^{-2} \\ \vdots \\ z_{av}^{-p} \end{pmatrix}, \tag{10}
$$

where superscript ^{T} stands for transposition.

In the general case, one can determine m coefficients of the basic approximating functions (not necessarily power polynomial) for the SF drift model and n coefficients of the basic approximating functions for the bias drift model. For this, it is necessary to obtain at least $p = m + n + 2$ equations, i.e. to simulate not less than p time intervals T of sign-changing virtual angle rate $\pm\Omega_v$. In this case, p equations for each gyroscope under calibration can be obtained.

Above, power polynomials have been used to approximate drift models for both parameters SF and bias. However, any types of basic approximation functions can be used for both SF and bias.

These equations, in the case of polynomial basic functions, in matrix form are represented as follows:

$$\vec{z}_{av} = M_p \left(SF_0 \quad a_{SF}^1 \quad \cdots \quad a_{SF}^m \quad B_0 \quad a_B^1 \quad \cdots \quad a_B^n \right)^{\mathrm{T}}, \quad (11)$$

where

$$\vec{z}_{av} = \left(z_{av}^{+1} \quad z_{av}^{-2} \quad \cdots \quad z_{av}^{p-1} \quad z_{av}^{p} \right)^{\mathrm{T}}, \; p = m + n + 2,$$

$$M_p = \begin{pmatrix} \Omega_v + \bar{\Omega}_1 & \cdots & \Omega_v + \bar{\Omega}_1 \dfrac{T^m}{m+1} & 1 & \dfrac{T}{2} & \cdots & \dfrac{T^n}{n+1} \\ \vdots & \vdots & \vdots & \vdots & \vdots & \vdots & \vdots \\ -\Omega_v + \bar{\Omega}_p & \cdots & -\Omega_v + \bar{\Omega}_p \dfrac{\left[p^m - (p-1)^m \right] T^m}{m+1} & 1 & \dfrac{(2p-1)T}{2} & \cdots & \dfrac{\left[p^n - (p-1)^n \right] T^n}{n+1} \end{pmatrix}.$$

Solution of equations (11) can be obtained by analogy with (10), where instead of M_1, M_p matrix is substituted. This solution yields a gyro scale factor SF_0 as well as its bias B_0 at the beginning of the calibration interval of pT duration and m coefficients $a_{SF}^1, a_{SF}^2, \cdots a_{SF}^m$ of the SF, and n coefficients $a_B^1, a_B^2, \cdots a_B^n$ of the bias polynomial models of mth and nth orders, respectively.

Figure 4 shows a graph of $p = m + n + 2$ time intervals of the simulated sign-changing virtual angle rates. These coefficients are used to determine a gyro scale factor and bias at the end of the current calibration interval as follows:

$$SF(pT) = SF_0 + a_{SF}^1 pT + a_{SF}^2 pT^2 + \cdots a_{SF}^m pT^m,$$
$$B(pt) = B_0 + a_B^1 pT + a_B^2 pT^2 + \cdots a_B^n pT^n. \quad (12)$$

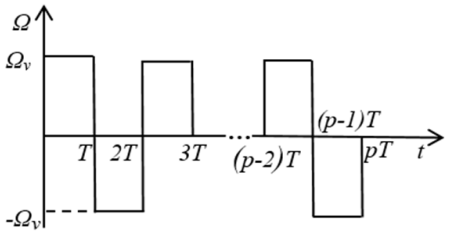

Fig. 4. Simulated sign-changing virtual angle rate

Using this periodic calibration, one can mitigate the requirement to the gyro SF and bias. In the case when an IMU consists of four gyros, the gyro requirement mitigation coefficient for per hour of motion may be equal to $K_m = 3600\ R\ /3pT$, where T is a time in seconds and R is a ratio of non-calibrated and calibrated gyro parameters error after each calibration period, respectively. This coefficient can also be interpreted as a coefficient of the gyro accuracy increasing undergoing such a periodic calibration. When an IMU consists of six, preferably MEMS gyros, K_m increases three times, because the time between the calibrations of the same gyro, in this case, is three times less, that is equal to pT.

Moreover, expressions (12) can also be used to predict SF and bias with the aim of angle rate correction during the measurement mode up to the beginning of the next calibration mode of this gyro, thus, increasing the requirement mitigation coefficient K_m.

To reduce the maximum degrees of the polynomial model of the SF and bias, it is necessary to reduce calibration time and simultaneously to reduce the gyro noise to obtain an accurate value of the averaged output signal z_{av} during shorter time interval T and, thus, to increase estimation accuracy of gyro parameters. Besides, the simulation error of the virtual angle rate Ω_v in the temperature range should also be minimum. All those results in the necessity to minimize calibration time pT to reduce degrees of the polynomial models.

It should be noted that to simulate a constant angle rate in the temperature range by providing a digital code or voltage to the gyroscope under calibration, it is necessary to compute which value of the digital code (or voltage) corresponds to a predetermined virtual angle rate Ω_v. Since this code (or voltage) depends on the temperature, one needs to have a temperature model by which this value of a code can be computed.

As has been discussed above, the more accurate approximation of the measurement data under temperature change is provided when including in the model additional parameters such as resonant frequency, drive (excitation), and quadrature amplitudes [14]. They are CVG control signals.

Figure 5 shows the digital code of one of the metallic resonator CVG samples that simulates a virtual constant angle rate of 100 deg/s at continuous changing of external temperature from –40°C to 75°C with a ramp of 1°C/min (black curve 1) and its approximating model (gray curve 2).

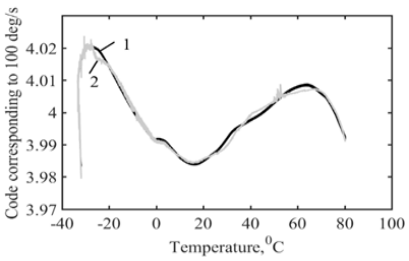

Fig. 5. Code that simulates a virtual angle rate 100 deg/s (1), and its approximation (2)

It should be noted that the digital code at the ADC output has been normalized so that it is numerically equal to the voltage in volts at the ADC input. The model depending on the four parameters is presented as follows [14]:

$$C = 4 - 0.066691 \times (f - f_0) + 0.024580 \times (f - f_0)^2 + 0.004832 \times (f - f_0)^3 + 11.309656 \times A_{dr} - 32.994747 \times A_{dr}^2 + 24.277287 \times A_{dr}^3 - 2.079236 \times A_q + 10.169294 \times A_q^2 - 13.167187 \times A_q^3 - 0.00225 \times t - 0.000144 \times t^2 + 0.0000009 \times t^3, \quad (13)$$

where C is a code that has to form the gyro processor to simulate 100 deg/s, f is a resonant frequency, f_0 = 4224.17 Hz is a reference frequency, A_{dr} is a drive amplitude, A_q is a quadrature amplitude and t is a temperature in degrees Celsius.

All these parameters (f, A_{dr}, A_q, and t), except f_0, by which the code is computed, are functions of time and temperature during a gyro operation. An RMS error of the code approximation by the four-parameter model is 0.025% and can be less when temperature change is less than 1°C/min.

VI. Proof-of-Concept Experiment

To simplify the experiment it is carried out at the constant room temperature, and a vehicle angle rate Ω_b is substituted by rotation of a turntable with a known angle rate. Figure 6 shows the metallic resonator vibratory gyroscope TVG-25 manufactured by the AT "Elmiz" company (Kyiv, Ukraine) on a rotating turntable. At these conditions, the proposed calibration method can be carried out for a single-axis gyro.

At the first stage, calibration and measurement are carried out in the absence of rotation, when Ω_b is equal to zero. A virtual angle rate Ω_v=±100 deg/s is simulated by the code ±3.9874, which is added to the output of controller 3 (see Fig. 1).

Figure 7 shows the output signal of the gyroscope when simulating a virtual angle rate of 100 deg/s with a sampling rate of 500 Hz. The average value of the output signal is 100.0179 deg/s, and the standard deviation of the noise is 0.0092 deg/s.

Fig. 6. Metallic resonator CVG mounted on a turntable to calibrate during rotation

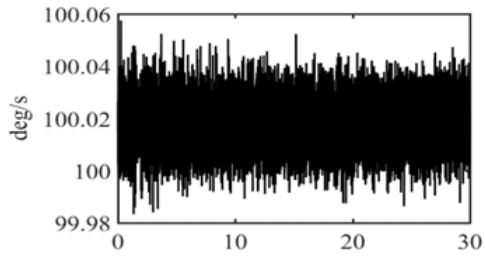

Fig. 7. Simulation of a virtual angle rate of 100 deg/s

Due to the constant temperature, the SF model is taken as a constant value $SF(t) = SF_0$. The gyro bias model is taken as a linear drift with noise, $B(t) = B_0 + +a_B t + \xi(t)$, where B_0 is the sum of the gyro bias at the beginning of the calibration mode and the vertical component of the Earth angle rate, a_B is the drift rate, and $\xi(t)$ is the gyroscope measurement noise.

Thus, to calculate the three parameters SF_0, B_0, and a_B, it is necessary to simulate at least three sign-changing angle rates (for $m = 0$ and $n = 1$, $p = m + n + 2 = 3$) in the calibration mode, each with a duration of T seconds, with total calibration time of $3T$.

In addition, the fourth interval of $3T$ duration is performed in the measurement mode. To compare the angle rate measurement errors, the values measured by the gyro are corrected by the SF and bias values calculated at the calibration mode. To correct the drift, a constant bias value calculated at the end of the calibration interval is used, as well as a linear drift prediction based on the adopted bias model following (12).

Figure 8 shows the output signal of the gyro, in which the virtual angle rate Ω_v = ± 100 deg/s is simulated when the angle rate of the real rotation Ω_b is equal to zero.

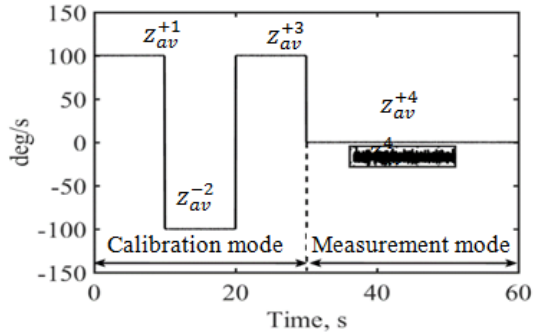

Fig. 8. Calibration with virtual angle rate ± 100 deg/s

Time interval T = 10 s is chosen. The average value of the gyro output signal for each T = 10 s time interval, designated on the graph, are: z_{av}^{+1}=100.0179 deg/s, z_{av}^{-2}= –99.9827 deg/s, and z_{av}^{+3}=100.0181 deg/s with virtual rotation in calibration mode and z_{av}^{+4}= 0.0183 deg/s in the measurement mode of a zero angle rate. The calibration mode consists of three 10-second intervals, and the measurement mode consists of one 30-second interval, during which, in a real IMU, three other gyros will be calibrated, in the case of a 6-gyro IMU, or one gyro in the case of a 4-gyro IMU.

For the SF and bias models adopted here, as a constant and linear function, respectively, equation (11) is written as follows:

$$\begin{aligned} \vec{z}_{av} &= M\begin{pmatrix} SF_0 & B_0 & a_B \end{pmatrix}^{\mathrm{T}}, \\ \vec{z}_{av} &= \begin{pmatrix} z_{av}^{+1} & z_{av}^{-2} & z_{av}^{+3} \end{pmatrix}^{T}, \end{aligned} \tag{14}$$

where the matrix M and the components of the vector $\vec{z}_{av}$ are as follows:

$$M = \begin{pmatrix} \Omega_v & 1 & \dfrac{T}{2} \\ -\Omega_v & 1 & \dfrac{3T}{2} \\ \Omega_v & 1 & \dfrac{5T}{2} \end{pmatrix} = \begin{pmatrix} 100 & 1 & 5 \\ -100 & 1 & 15 \\ 100 & 1 & 25 \end{pmatrix}, \tag{15}$$

$$\vec{z}_{av} = \begin{pmatrix} 100.0179 & -99.9827 & 100.0181 \end{pmatrix}^{\mathrm{T}}.$$

Solution of this equation gives the following calibration values for the three parameters: SF_0 = 1.0000036 LSB/(deg/s), where LBS is a least significant bit; B_0 = 0.0174 deg/s; a_B = 1.5×10^{-5} deg/s^2.

In this case, the average values of the virtual angle rate ± 100 deg/s at each of the three 10-second intervals, after their correction, are equal to, respectively:

$$\begin{aligned} \Omega_{av}^{+1} &= \frac{z_{av}^{+1}}{SF_0} - \left(B_0 + a\frac{T}{2} \right) = 100.000065 \text{ deg/ s}, \\ \Omega_{av}^{-2} &= \frac{z_{av}^{-2}}{SF_0} - \left(B_0 + a\frac{3T}{2} \right) = -99.999965 \text{ deg/ s}, \\ \Omega_{av}^{+3} &= \frac{z_{av}^{+3}}{SF_0} - \left(B_0 + a\frac{5T}{2} \right) = 99.999965 \text{ deg/ s}. \end{aligned} \tag{16}$$

Thus, the simulation error of the virtual angle rates in the calibration mode is ± 0.000035 deg/s = ± 0.126 deg/h.

Then, the parameters obtained in the calibration mode are used to correct the angle rate in the measurement mode. The measuring mode lasts 30 s, at which the true angle rate is zero. The correction is performed by subtracting a constant bias value obtained at the end of the calibration interval, i.e. at the end of the 30th second. The average value of the angle rate in the measurement mode can be calculated using the following expression:

$$\begin{aligned} \bar{\Omega}_{av}^{corr} &= \frac{z_{av}^4}{SF_0} - (B_0 + 3a_B T) = \frac{0.0183}{1.0000036} \\ -0.0174 + 0.00045 &\approx 4.5\times10^{-4} \text{ deg/ } s \approx 1.6 \text{ deg/ h}. \end{aligned} \tag{17}$$

As the real angle rate is zero, the measurement error after correction is $\Delta\bar{\Omega}_{av}^{corr}$ = 1.6 deg/h.

Note that the average value of the non-corrected angle rate in the measurement interval is z_{av}^4 = 0.0183 deg/s ≈65.88 deg/h. The mitigation factor for the gyroscope is R = 65.88/1.6 ≈ 41.

When correcting the drift using the prediction on the measurement interval, we get the following result:

$$\begin{aligned} \bar{\Omega}_{av}^{pred} &= \frac{z_{av}^4}{SF_0} - (B_0 + 9a_B T/2) \\ &\approx 2.25\times10^{-4} \text{ deg/ s} \approx 0.81 \text{ deg/ h}. \end{aligned} \tag{18}$$

The measurement error of the zero angle rate when using the drift prediction in the measurement interval is decreased almost 2 times and, accordingly, the coefficient K_m is also increased.

Thus, when using the prediction, the coefficient K_m may increase. However, if the drift in the measurement interval changes, i.e. coefficient a_B in the adopted model, the prediction will lead to a decrease in K_m coefficient. Accordingly, this results in a decrease of the angle rate measurement accuracy as compared to the correction by expression (17), where the constant value of the bias obtained at the end of the calibration interval is used.

Figure 9 shows the second stage of the experiment, where the gyroscope in the calibration and measurement modes rotates with an angle rate of Ω_b = 50 deg/s.

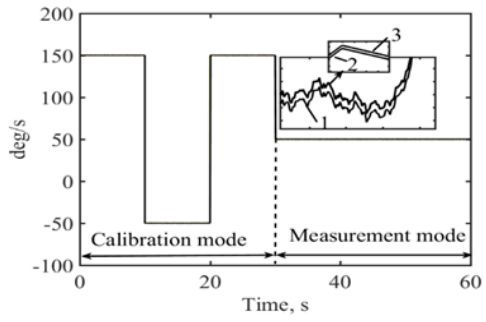

Fig. 9. Calibration and correction when measuring angle rate 50 deg/s

At the first calibration time interval of T = 10 s duration, the gyro measures the sum of two angle rates $\Omega_v + \Omega_b$ = 150 deg/s, at the second one it measures the difference $-\Omega_v + \Omega_b = -50$ deg/s, and at the third one, it again measures the sum $\Omega_v + \Omega_b$ = =150 deg/s. The third interval ends the calibration mode. In the measurement mode Ω_v = 0, and the gyro measures only Ω_b = 50 deg/s.

Figure 9 shows a magnified fragment of the measurement mode. Curve 1 is the output signal of the gyro. Curve 2 is the output signal of the gyro, corrected by subtracting the constant value of the bias obtained at the end of the 30th second of the calibration interval. Curve 3 is the gyro output signal corrected by the drift prediction on the measurement interval. The values of the angle rate and their errors in the measurement mode are equal to $\bar{\Omega}_{av}^{corr}$ = = 49.999008 deg/s, i.e. measurement error is $\Delta\bar{\Omega}_{av}^{corr}$ = 0.000992 deg/s≈3.57 deg/h, when corrected by the expression (17), and $\bar{\Omega}_{av}^{pred}$ = 50.0039 deg/s, i.e. error is $\Delta\bar{\Omega}_{av}^{pred}$ = 0.0039 deg/s = 14.04 deg/h, when corrected by the expression (18).

VII. Discussion of Measurement Errors

Thus, when measuring the angle rate of 50 deg/s, the measurement error when corrected using the drift prediction increases in comparison with the correction based on the drift value at the end of the calibration interval. Possible reasons for the worsening in measurement accuracy are a significant increase in noise and a change in drift parameters.

Figure 10 shows the output signal of the gyro when measuring the turntable angle rate of 50 deg/s.

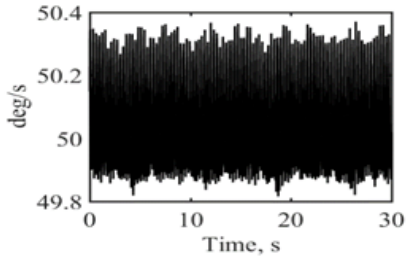

Fig. 10. The turntable angle rate 50 deg/s, measured by the gyro

The average value of the gyro output signal is 50.0322 deg/s. The noise of the signal shown in fig. 10 consists of the gyro measurement noise and the short-term periodic noise of the turntable (with the period much less than the rotation period), due to the operation of the controller stabilizing the period of rotation. The RMS value of the total noise is 0.14 deg/s and is mainly determined by the noise of the turntable, since the RMS of the gyro noise, as indicated above, is σ = 0.0092 deg/s (see Fig.7).

In the computations presented in subsection *V*, it was assumed that the errors of Ω_b, and Ω_v were equal to zero, i.e. into the matrix M of equation (15) the values Ω_b = 0, Ω_b = 50 deg/s, and Ω_v = ±100 deg/s are substituted. However, as follows from Fig. 5, simulation of the angle rate at different temperatures will have an error. The angle rate Ω_b has an error, as well. This error was computed above in cases of correction by the value of the bias obtained at the end of the calibration interval and using the prediction.

Figure 11 presents a graph of the ratio R, which is a ratio of non-calibrated and calibrated gyro after each calibration period versus the measurement error $\Delta\Omega_b$ of the angle rate and the simulation error $\Delta\Omega_v$ of the virtual angle rate for the above linear model of the gyroscope error adopted above. As can be seen from the graph, the minimum value of R=10 with errors of both parameters $\Delta\Omega_b$ and $\Delta\Omega_v$ varying in the range of no more than ± 20 deg/h. This means that at each step of the periodic calibration with duration of 30 s, the angle rate measurement error decreases by at least 10 times relative to the current gyro error without calibration.

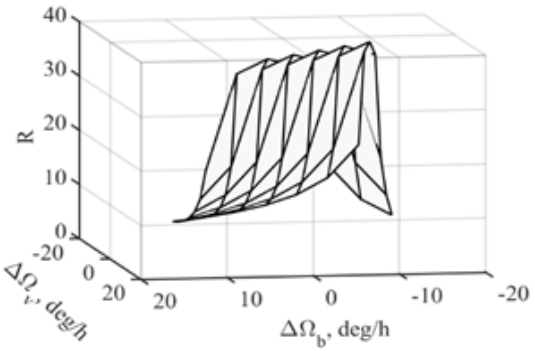

Fig. 11. The dependence of a ratio R on measurement and virtual angle rate errors

The behavior of the angle rate error accumulation versus time, under the condition of a constant linear drift, which is possible with a linear temperature change and using for correction a constant value of the bias at the end of each calibration interval, can be represented as shown in Fig. 12.

In Figure 12, straight line 1 represents the behavior of the angle rate error accumulation with a linear bias drift of a non-calibrated gyro, and broken line 2 represents an error accumulation of periodically calibrated gyro. It is clear from the graph that the more often the calibration is performed, the less the accumulated error with compared to a non-calibrated gyro. Therefore, ratio R increases and, together with it, gyro requirements mitigation coefficient K_m increases, as well.

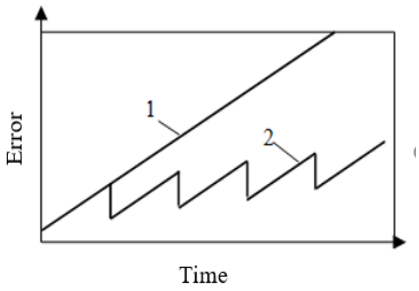

Fig. 12. The behavior of error accumulation under periodical calibration

VII. CONCLUSIONS

Thus, to maximize the gyro requirements mitigation coefficient K_m in a redundant IMU, it is necessary to reduce the gyro measurement noise, which results in reduction of a calibration time, as well as the time between calibrations.

To minimize the time interval between calibrations, a 6-gyro IMU should be used, as the proposed calibration method can be applied to several gyros at the same time.

To improve calibration accuracy at higher gyro noise, the simulated virtual angle rate Ω_v should exceed the vehicle's maximum angle rate Ω_b as much as possible.

To reduce the influence of measurement noise on the calibration accuracy, redundant measurements following expressions (9) and (10) can also be used.

In addition, within the framework of the proposed calibration method, it is possible to change the models of SF and bias errors at each next calibration depending, for example, on the environment rate of a temperature change or other conditions.

REFERENCES

[1] D. Titterton and J. Weston, "Strapdown Inertial Navigation Technology," The American Institute of Aeronautics and Astronautics, second edition, 2004. https://doi.org/10.1049/PBRA017E

[2] Oliver J. Woodman, "An introduction to inertial navigation," Technical Report, N. 696, UCAM-CL-TR-696, ISSN 1476-2986, UK, University of Cambridge, August, 2007, p. 37.

[3] S. Nassar, "Improving the Inertial Navigation System (INS) Error Model for INS and INS/DGPS Applications," Ph.D. Thesis, University of Calgary, Calgary, AB, Canada, 2003.

[4] Q. Honghui and J. B. Moore, "Direct Kalman filtering approach for GPS/INS integration," *IEEE Transactions on Aerospace and Electronic Systems*, vol. 38, Issue: 2, Apr, 2002, pp. 687–693. https://doi.org/10.1109/TAES.2002.1008998

[5] B. Johan and S. Willem, "Kalman filter configurations for a low-cost loosely integrated inertial navigation system on an airship," *Control Engineering Practice*, vol. 16, Issue 12, Dec, 2008, pp. 1509–1518. https://doi.org/10.1016/j.conengprac.2008.04.011

[6] A. Noureldin, T. B. Karamat, M. D. Eberts, and A. El-Shafie, "Performance Enhancement of MEMS-Based INS/GPS Integration for Low-Cost Navigation Applications," *IEEE Transactions on Vehicular Technology*, vol. 58, Issue 3, March, 2009, pp. 1077–1096. https://doi.org/10.1109/TVT.2008.926076

[7] V. V. Chikovani, "Laser device for three-axis orientation measurement with low sensitivity to gyro errors (computer simulation results)," *Proc. SPIE Optical Engineering*, vol. 34, no. 4, 1995, pp. 1008–1012. https://doi.org/10.1117/12.197150

[8] J. Ban, L. Wang, Z. Liu, and L. Zha, "Self-calibration method for temperature errors in multi-axis rotational inertial navigation system," *Optics Express*, vol. 28, no. 6/16, March, 2020, pp. 8909–8922. https://doi.org/10.1364/OE.384905

[9] Q. Ren, B. Wang, Z., and M. Fu, "A multi-position self-calibration method Deng for dual-axis rotational inertial navigation system," *Sensors and Actuators A*, 219, 2014, pp. 24–31. https://doi.org/10.1016/j.sna.2014.08.011

[10] P. Gao, K. Li, L. Wang, and Z. Liu, "A self-calibration method for tri-axis rotational inertial navigation system," *Measurement Science and Technology*, vol. 27, Oct., no. 11, 2016. https://doi.org/10.1088/0957-0233/27/11/115009

[11] D. M. Rozelle, "Self-calibrating gyroscope system," US Patent # 7912664, G01C 19/00, 22 March, 2011.

[12] G. Casinovi, F. Ayazi, W. K. Sung, M. J. Dalal, A. N. P. Shirazi, "Method and apparatus for self-calibration of gyroscopes," US Patent #9915532, G01C 25/00, 19/5776, 19/56, 13 March, 2018.

[13] H. Gu, B. Zhao, H. Zhou, X. Liu, and W. Su, "MEMS Gyroscope Bias Drift Self-Calibration Based on Noise-Suppressed Mode Reversal," *Micromachines*, 10, 823, 2019, pp. 1–17; https://doi.org/10.3390/mi10120823.

[14] V. V. Chikovani and O. V. Petrenko, "Vibratory gyroscope scale factor multi-parametric calibration," *IEEE Proc. Intern. Conf. on Methods and Systems of Navigation and Motion Control (MSNMC)*, NAU, Kyiv, Ukraine, Oct.14-17, 2014, pp. 129–131. https://doi.org/10.1109/MSNMC.2014.6979750

[15] V. Chikovani, H. Tsiruk, and O. Korolova, "Triple-Mode Vibratory Gyroscope," *Military Technical Collection*, Hetman Petro Sahaidachnyi National Army Academy, Lviv, Ukraine, no. 18, 2018, pp. 18–24. https://doi.org/10.33577/2312-4458.18.2018.18-25

Received August 29, 2021.

Chikovani Valeri. ORCID 0000-0003-1436-7180. Doctor of Engineering Sciences. Professor.
Aerospace Control Systems Department, Faculty of Air Navigation Electronics and Telecommunications, National Aviation University, Kyiv, Ukraine
Education: Moscow Physical-Technical Institute, Moscow, Russia, 1975.
Research area: Gyroscopes, Inertial Measurement Units, Navigation, Control Systems.
Publications: more than 100
E-mail: v_chikovani@ukr.net

Golovach Serhii. ORCID 0000-0001-6786-3781. Candidate of Engineering Sciences. Chief designer of gyroscopic and navigation systems.
JSC Elmiz Kyiv, Ukraine
Education: National Technical University of Ukraine "Igor Sikorsky Kyiv Polytechnic Institute", Kyiv, Ukraine, (2013)
Research area: Gyroscopes, Inertial Measurement Units, Navigation, Control Systems.
Publications: more than 25
E-mail: golovach.s@meta.ua

В. В. Чіковані, С. В. Головач. Самокалібрування масштабних коефіцієнтів та зміщень нуля вібраційних гіроскопів у русі

Пропонується новий спосіб періодичного самокалібрування масштабного коефіцієнта і зміщення нуля вібраційних гіроскопів у русі в інерціальному вимірювальному блоці з надмірною кількістю датчиків. Самокалібрування використовує заздалегідь задані віртуальні позитивні і негативні кутові швидкості для калібрування масштабного коефіцієнта та зміщення нуля гіроскопу, що калібрується, у той час як інші не менше трьох гіроскопів в інерційному вимірювальному блоці працюють у режимі вимірювання реальної кутової швидкості об'єкту. Проекція поточної кутової швидкості на вісь чутливості гіроскопу, що калібрується обчислюється за результатами вимірювання повного вектору кутової швидкості іншими трьома гіроскопами, створюючи умови для процедури калібрування. На відміну від відомих способів, таких як одно- або багатовісного обертання інерційного вимірювального блоку і реверсу мод коливань, запропонований спосіб не використовує механічне обертання, що вимагає додаткових пристроїв, а також не вимагає переорієнтацію вібраційної хвилі, що викликає необхідність вирівнювання параметрів двох вимірювальних каналів. Процедура калібрування масштабного коефіцієнта і зміщення нуля за цим способом може застосовуватися для декількох гіроскопів одночасно. Запропонований спосіб має велику перспективу застосування не тільки для малогабаритних 4-гіроскопних інерціальних вимірювальних блоків і для багато-гіроскопних інерціальних вимірювальних блоків, побудованих на гіроскопах на основі мікро-електро-механічних систем. Експериментально показано, що використовуючи запропонований спосіб, коефіцієнт послаблення вимог до гіроскопа може бути збільшений і може забезпечити високу точність для автономної навігації на дешевих малогабаритних та мікро-електро-механічних гіроскопах.

Ключові слова: масштабний коефіцієнт; дрейф; віртуальна кутова швидкість; самокалібрування; коефіцієнт послаблення.

Валерій Валеріанович Чіковані. ORCID 0000-0003-1436-7180. Доктор технічних наук. Професор.
Кафедра аерокосмічних систем управління, Факультет аеронавігації, електроніки та телекомунікацій. Національній авіаційний університет, Київ, Україна.
Освіта: Московський фізико-технічний інститут, 1975.
Напрям наукової діяльності: гіроскопи, інерційні вимірювальні блоки, навігація, системи управління.
Кількість публікацій: більше 100 наукових робіт.
E-mail: v_chikovani@ukr.net

Сергій Володимирович Головач. ORCID 0000-0001-6786-3781. Кандидат технічних наук. Головний конструктор гіроскопічних та навігаційних систем.
АТ Елміз, Київ, Україна.
Освіта: Національний технічний університет України «Київський політехнічний інститут ім. І. Сікорського», Київ, Україна, 2013.
Напрям наукової діяльності: гіроскопи, інерційні вимірювальні блоки, навігація, системи управління.
Кількість публікацій: більше 25 наукових робіт.
E-mail: golovach.s@meta.ua

В. В. Чиковани, С. В. Головач. Самокалибровка масштабного коэффициента и смещения нуля вибрационного гироскопа в движении

Предлагается новый способ периодической самокалибровки масштабного коэффициента и смещения нуля вибрационных гироскопов в движении в инерциальном измерительном блоке с избыточным количеством датчиков. Самокалибровка использует заранее заданные виртуальные положительные и отрицательные угловые

скорости для калибровки масштабного коэффициента, и смещения нуля гироскопа, который находится в режиме калибровки, в то время как другие не менее трех гироскопов в инерциальном измерительном блоке работают в режиме измерения реальной угловой скорости объекта. Проекция текущей угловой скорости на ось чувствительности калибруемого гироскопа вычисляется по результатам измерения полного вектора угловой скорости другими тремя гироскопами, создавая условия для процедуры калибровки. В отличие от известных способов, таких как одно- или многоосное вращение инерциального измерительного блока и реверса мод колебаний, предлагаемый способ не использует механическое вращение, что требует дополнительных устройств, и не требует переориентации вибрационной волны, что влечет за собой необходимость выравнивания параметров двух измерительных каналов. Процедура калибровки масштабного коэффициента и смещение нуля по этому способу может применяться для нескольких гироскопов одновременно. Поэтому предлагаемый способ имеет большую перспективу применения для малогабаритных 4-гироскопных инерциальных измерительных блоков и для многогироскопных инерциальных измерительных блоков, построенных на гироскопах, основанных на микро-электро-механических гироскопах. Экспериментально показано, что используя предложенный способ, коэффициент ослабления требований к гироскопу может быть увеличен и может обеспечить высокую точность для автономной навигации на дешевых малогабаритных и микро-электро-механических гироскопах.

Ключевые слова: масштабный коэффициент; дрейф; виртуальная угловая скорость; самокалибровка; коэффициент ослабления.

Валерий Валерианович Чиковани. ORCID 0000-0003-1436-7180. Доктор технических наук. Профессор.
Кафедра аэрокосмических систем управления, Факультет аэронавигации, электроники и телекоммуникаций, Национальный авиационный университет, Киев, Украина.
Образование: Московский физико-технический институт, 1975.
Направление научной деятельности: гироскопы, инерциальные измерительные блоки, навигация, системы управления.
Количество публикаций: больше 100 научных робот.
E-mail: v_chikovani@ukr.net

Сергей Владимирович Головач. ORCID 0000-0001-6786-3781. Кандидат технических наук. Главный конструктор гироскопических и навигационных систем.
АО Элмиз, Киев, Украина.
Образование: Национальный технический университет Украины «Киевский политехнический институт им. И. Сикорского», Киев, Украина, 2013.
Направление научной деятельности: гироскопы, инерциальные измерительные блоки, навигация, системы управления
Количество публикаций: больше 25 научных робот.
E-mail: golovach.s@meta.ua